Published in final edited form as:
Virology. 2013 November ; 446(0): 251–259. doi:10.1016/j.virol.2013.08.013.

Human Papillomavirus Type 16 E7 oncoprotein inhibits the anaphase promoting complex/cyclosome activity by dysregulating EMI1 expression in mitosis

Yueyang Yu and **Karl Munger**[#]
Division of Infectious Diseases, Brigham and Women's Hospital and Biological and Biomedical Sciences Program, Harvard Medical School, Boston, Massachusetts, 02115

Abstract

The anaphase promoting complex/cyclosome (APC/C) is a ubiquitin ligase complex that orchestrates mitotic progression by targeting key mitotic regulators for proteasomal degradation. APC/C dysfunction is a frequent event during cancer development and can give rise to genomic instability. Here we report that the HPV16 E7 oncoprotein interferes with the degradation of APC/C substrates and that the APC/C inhibitor, EMI1, is expressed at higher levels in HPV16 E7-expressing mitotic cells. HPV16 E7 expression causes increased EMI1 mRNA expression and also inhibits EMI1 degradation. The resulting abnormally high EMI1 levels in HPV16 E7-expressing mitotic cells may inhibit degradation of APC/C substrates and cause the prometaphase delay that we have previously observed in such cells.

Keywords

Human Papillomaviruses; E7 oncoprotein; Mitosis; Anaphase Promoting Complex/Cyclosome (APC/C); EMI1; Genomic Instability; Cervical Cancer

INTRODUCTION

Ubiquitin-mediated degradation of cellular proteins constitutes an essential mechanism to tightly regulate steady state levels of proteins and their biological activities in a cell. The selectivity of ubiquitylation is achieved by ubiquitin-protein ligases (E3s), among which the anaphase promoting complex/cyclosome (APC/C) serves as a master regulator of mitotic progression as well as DNA replication licensing in G1. The APC/C complex is composed of over a dozen subunits and the CDC20 and CDH1 co-activators confer activation and some degree of substrate specificity during the somatic cell cycle (Peters, 2006). The APC/C^{CDC20} complex becomes active in early mitosis and targets securin and cyclin B for degradation, which is required for sister chromatid separation and mitotic exit. From late mitosis to G1, the APC/C^{CDH1} complex forms and replaces APC/C^{CDC20} by ubiquitylating CDC20. APC/C^{CDH1} also targets other mitotic regulators including Polo-like kinase 1 (PLK1) and Aurora kinases for degradation. These sequential waves of APC/C substrate

[#]Corresponding author. Mailing Address: 181 Longwood Ave., MCP 861, Boston, MA 02215. Phone (617) 525-4282, Fax (617) 525-4283, kmunger@rics.bwh.harvard.edu.

degradation drive many events during mitotic progression including sister chromatid separation and cytokinesis (Pines, 2011).

Since premature degradation of APC/C substrates such as securin and cyclin B increases the risk of chromosome segregation errors, there are several mechanisms that control APC/C activity. The mitotic spindle assembly checkpoint (SAC) inhibits APC/C^{CDC20} activity until chromosomes are attached to microtubules and aligned at the metaphase plate (Musacchio and Salmon, 2007). However, APC/C^{CDC20} targets cyclin A and NEK2A for degradation right after nuclear envelope breakdown despite the activation of the SAC (van Zon and Wolthuis, 2010). There are also SAC-independent inhibitors of the APC/C. The Ras association domain-containing family 1 isoform A (RASSF1A) protein and RAE1-NUP98 are thought to inhibit the early mitotic APC/C, whereas early mitotic inhibitor 1 (EMI1) has been reported to inhibit both the mitotic APC/C^{CDC20} and the interphase APC/C^{CDH1} complexes (Di Fiore and Pines, 2007; Hsu et al., 2002; Jeganathan et al., 2005; Margottin-Goguet et al., 2003; Reimann et al., 2001a; Song et al., 2004).

Given its essential roles in regulation of chromosome segregation and DNA replication, dysregulation of the APC/C activity has been linked to genomic instability and cancer development in many ways (Lipkowitz and Weissman, 2011; Nakayama and Nakayama, 2006). Studies with mouse models, for example, have established a clear link between SAC dysfunction and aneuploidy (Suijkerbuijk and Kops, 2008). CDH1 functions as a haploinsufficient tumor suppressor and reduced CDH1 expression impairs genetic stability (Engelbert et al., 2008; Garcia-Higuera et al., 2008). Overexpression of APC/C substrates such as cyclin A, cyclin B, Aurora A, PLK1, TPX2, CDC6, or SKP2 are also associated with chromosomal instability and are predictors of poor prognosis in human cancers (Carter et al., 2006).

High-risk mucosal human papillomaviruses (HPVs) are small DNA viruses that are causative of most cervical cancers and a significant portion of other anogenital tract and oral carcinoma (McLaughlin-Drubin et al., 2012). They infect squamous mucosal epithelia and maintain their genomes as episomes in the basal cell layer. The productive phase of the viral life cycle occurs exclusively in differentiated cells. E6 and E7 are two low molecular size viral proteins that are consistently expressed in HPV-associated cancers. They lack intrinsic enzymatic activities and contribute to the induction and maintenance of the transformed phenotype through protein-protein interactions (Klingelhutz and Roman, 2012; Moody and Laimins, 2010; Munger et al., 2004). Interestingly, the major transforming activities of the high-risk HPV16 E6 and E7 proteins have been linked to the proteolytic inactivation of tumor suppressors p53 and pRB by reprogramming the cellular ubiquitin ligase E6AP and the CUL2-containing cullin RING ligase complex, respectively (Huh et al., 2007; Scheffner et al., 1993; White et al., 2012).

In addition to uncoupling the host cell differentiation program from proliferation by dysregulating the pRB/E2F axis, HPV16 E7 drives genomic destabilization (McLaughlin-Drubin and Munger, 2009a, b). Double stranded DNA breaks and anaphase bridges are observed at a higher frequency in HPV16 E7-expressing cells than in control cells (Duensing and Munger, 2002). Expression of HPV16 E7 also induces centrosome overduplication and increases the risk for multipolar mitoses and chromosome missegregation (Duensing et al., 2000). In fact, multipolar mitoses are histopathological hallmarks of high-risk HPV-associated premalignant lesions and cancers (Winkler et al., 1984). Furthermore, HPV16 E7-expressing cells progress more slowly through prometaphase as originally detected by live cell videomicroscopy (Nguyen and Munger, 2009). More recent studies revealed that degradation of APC/C substrates including cyclin A and cyclin B is inhibited in HPV16 E7-expressing cells (Yu and Munger, 2012). Although

HPV16 E7 expression triggering the SAC may account for inhibition of cyclin B degradation, this mechanism cannot account for the inhibition of cyclin A degradation (Yu and Munger, 2012). Hence, HPV16 E7 may also negatively regulate APC/C activity through SAC-independent mechanisms.

In this report, we examine the degradation of a range of different APC/C substrates during mitotic progression and find that HPV16 E7 can be added to an expanding list of viral proteins that manipulate the APC/C (Fehr and Yu, 2013; Heilman et al., 2005; Mo et al., 2012). The SAC-independent APC/C inhibitor, EMI1, is an E2F transcriptional target (Hsu et al., 2002) and is not only transcriptionally upregulated by HPV16 E7, but the EMI1 protein is also stabilized during mitosis. Furthermore, EMI1 depletion partially reverses the inhibition of APC/C substrate degradation in HPV16 E7-expressing cells. The discovery that HPV16 E7 targets the APC/C inhibitor, EMI1, suggests that the inhibition of APC/C activity may play important roles in E7-induced mitotic abnormalities.

RESULTS

HPV16 E7 expression affects APC/C substrate degradation during mitosis

We have previously reported that HPV16 E7 expression impedes the degradation of the mitotic APC/C substrates cyclin A and cyclin B (Yu and Munger, 2012). While inhibition of the SAC partially restores cyclin B degradation in HPV16 E7-expressing cells, the inhibition of degradation of cyclin A, an APC/C^{CDC20} substrate not regulated by the SAC, remains unaffected. Thus we decided to pursue the possibility that HPV16 E7 may inhibit APC/C activity independent of the SAC and hence may impede the degradation of other APC/C substrates as well. To address this, we examined three distinct categories of APC/C substrates: (a) Cyclin A and NEK2A are degraded after nuclear envelope breakdown by the APC/C^{CDC20} complex and therefore evade control by the SAC (van Zon and Wolthuis, 2010); (b) Cyclin B and securin are the best-characterized APC/C^{CDC20} substrates that are degraded only after the SAC is satisfied by proper microtubule attachment to the kinetochores; (c) CDC20, PLK1, and Aurora B are ubiquitylated by the APC/C^{CDH1} complex after anaphase (Pines, 2011).

Primary human foreskin fibroblasts (HFFs) were used for these experiments as, unlike keratinocytes, they are amenable to the double thymidine synchronization scheme. We generated donor and passage matched primary HFF populations retrovirally transduced with empty vector (HFF C) or HPV16 E7 (HFF E7) and assessed E7 expression by Western blotting (data not shown). HFF C and HFF E7 populations were arrested at the G1/S boundary by a double thymidine block and then released and followed through S and G2 phases and mitosis. We harvested cells and measured mitotic indices by two-dimensional FACS analyses to assess DNA content with propidium iodide staining and expression of the mitotic marker MPM-2. A mitotic peak was observed between 8 and 10 hours after release in both HFF C and HFF E7 (Fig 1A) and most of the cells passed through mitosis between 8 and 14 hours after release. We consistently observed a noticeably smaller decrease between 8 and 14 hours after release in levels of all three categories of APC/C substrates in HFF E7 than in HFF C. For the APC/C^{CDC20} substrates that are degraded independent of SAC activation, cyclin A levels decreased by 93% in HFF C but only by 56% in HFF E7, and NEK2A levels decreased by 85% in HFF C and only by 45% in HFF E7. For the APC/C^{CDC20} substrates that are only degraded after the SAC is turned off, cyclin B levels decreased by 98% in HFF C and by 75% in HFF E7, and securin levels decreased by 76% in HFF C and by 35% in HFF E7 (Fig 1A and 1B). Similar differences were also observed with APC/C^{CDH1} substrates. CDC20 levels declined by 52% in HFF C and by 16% in HFF E7, PLK1 levels declined by 36% in HFF C and by 21% in HFF E7, and Aurora B levels declined by 80% in HFF C and by 58% in HFF E7.

To determine whether some of these observed differences may be caused by differences in the proliferative activity between the two cell populations, we performed immunofluorescence analyses of the proliferation marker Ki67 in HFF C and HFF E7. 85% of HFF C and 86% of HFF E7 were Ki67-positive (n=200) (Fig 1C). Hence the proliferative activity of HFF E7 is similar to that of HFF C. Thus, the observed differences in APC/C substrate levels during mitosis do not reflect differences in proliferative activity but are consistent with the model that E7 may inhibit APC/C activity during mitosis.

HPV16 E7-expressing cells maintain high EMI1 levels during mitosis

Increased steady state levels of all three categories of APC/C substrates in mitotic HFF E7 populations led us to search for an SAC-independent APC/C inhibitor that may account for these differences. EMI1 was an attractive candidate as it has been shown to inhibit the mitotic APC/C^{CDC20} and unlike the SAC component MAD2, it can stabilize cyclin A in *Xenopus* egg extracts (Reimann et al., 2001b). The mechanisms by which EMI1 inhibits APC/C involve inhibition of both substrate binding and ubiquitin chain elongation as suggested by biochemical and structural studies (Frye et al., 2013; Miller et al., 2006; Wang and Kirschner, 2013). EMI1 accumulates at the G1/S transition due to E2F-mediated transcriptional upregulation and is targeted for degradation by the TrCP-containing SKP1/CUL1/F-box protein (SCF^{TrCP}) ubiquitin ligase at the onset of mitosis. EMI1 ubiquitylation by SCF^{TrCP} requires prior phosphorylation by PLK1 and CDK1 (Hansen et al., 2004; Hsu et al., 2002; Margottin-Goguet et al., 2003; Moshe et al., 2004). Moreover, since E7 dysregulates E2F activity EMI1 mRNA expression may be generally increased in HFF E7 populations. Hence, we examined modulation of EMI1 protein levels specifically during mitosis.

HFF E7 and HFF C were arrested at the G1/S boundary with a double thymidine block and then released into nocodazole, a spindle poison that triggers SAC activation and arrests cells in mitosis. Assessment of mitotic markers, the slower migrating phosphorylated form of CDC27 (indicated by an asterisk) and serine 10 phosphorylated histone H3 (H3-pS10), by Western blotting and mitotic indices measured by FACS, confirmed that both HFF C and HFF E7 populations were enriched in mitosis between 8 and 14 hours after release from the second thymidine block into nocodazole (Fig 2A). During this time, there was a 77% decrease in cyclin A levels and an 88% decrease in NEK2A levels in HFF C (Fig 2A and 2B), consistent with the model that cyclin A and NEK2A degradation are not affected by SAC engagement. On the other hand, cyclin B levels remained high in both HFF C and HFF E7 due to SAC activation. Similar to the results in synchronized, actively cycling cells (Fig 1), there was some stabilization of cyclin A and NEK2A in HFF E7, with a 9% decrease in cyclin A levels and a 62% decrease in NEK2A levels in HFF E7 as compared to HFF C.

Interestingly, while EMI1 levels were decreased by 89% between 8 and 14 hours after release into nocodazole in HFF C, they only decreased by 14% in HFF E7 (Fig 2A and 2B). These differences in EMI1 protein levels during mitosis suggest the possibility that E7 may perturb EMI1 ubiquitylation by SCF^{TrCP}. Since SCF^{TrCP} ubiquitylation of EMI1 requires prior phosphorylation by PLK1 (Hansen et al., 2004; Moshe et al., 2004), we examined PLK1 levels and PLK1 phosphorylation of cyclin B at serine 133 as a readout of PLK1 activity (Jackman et al., 2003) and did not detect major differences in HFF C and HFF E7. To investigate whether E7 may more generally inhibit SCF^{TrCP} activity, we also examined protein levels of the CDK1 inhibitory kinase WEE1A that is targeted for degradation by SCF^{TrCP} at the onset of mitosis (Watanabe et al., 2005). WEE1A levels decreased by 25% in HFF E7 as compared to 81% in HFF C. We also examined another classical SCF^{TrCP} substrate, β-catenin (Nakayama and Nakayama, 2005), but did not observe noticeable modulation of β-catenin levels in either HFF C or HFF E7 in our timecourse experiments (data not shown).

It should be noted that our quantifications of EMI1 band intensities normalized to actin were only relative to the 8 hour sample within their own group, HFF C or HFF E7, and that EMI1 protein levels were consistently 1.5 fold and 1.4 fold higher in HFF E7 than in HFF C at 0 and 8 hours after release, respectively. This general increase in EMI1 steady state levels may be due to dysregulated E2F transcriptional activity in HFF E7. In order to rule out the possibility that differences in the decrease of EMI1 protein levels are only due to differences in mRNA levels, we performed quantitative reverse transcription polymerase chain reaction (qRT-PCR) experiments (Fig 2C). Indeed, EMI1 mRNA levels were higher in HFF E7 at all time points examined compared to HFF C. EMI1 mRNA levels, however, declined similarly during mitosis, by 58% in HFF C and by 50% in HFF E7. The 8% difference in reduction in mRNA levels between HFF C and HFF E7, however, was much smaller than the 75% difference in the decrease of EMI1 protein levels in the two cell populations. Hence, HPV16 E7 may interfere with EMI1 protein degradation during mitosis.

EMI1 half-life during mitosis is increased in HPV16 E7-expressing human cells

In order to directly assess whether HPV16 E7 may affect EMI1 protein stability during mitosis, we performed a cycloheximide chase experiment analyzing endogenous EMI1 in nocodazole arrested mitotic cells (Fig 3). Given the overall lower EMI1 levels in HFF C, twice the lysate for HFF C was run on the gel to make the starting EMI1 levels more comparable to those in HFF E7 (Fig 3A). Quantification of EMI1 levels normalized to actin is shown in Fig 3B and EMI1 half-life was almost doubled from ~1 hour in HFF C to ~2 hours in HFF E7. However, we could not assess WEE1A half-life in the time frame examined in Fig 3.

In addition to HPV16 E7-expressing HFF populations, we also assessed levels of EMI1 expression in two independent populations of human foreskin keratinocytes (HFKs), the relevant host cell type for HPV infection. In each of the HPV16 E7-expressing populations, EMI1 levels were significantly higher than in matched control vector infected cells (Fig 3C). These results are consistent with the results obtained with HPV16 E7-expressing primary human fibroblasts.

MLN4924 has less stabilizing effects on EMI1 in HPV16 E7-expressing cells

In order to determine whether EMI1 stability is increased in HFF E7 as a consequence of perturbed SCF^{TrCP}-mediated ubiquitylation, we examined the effects of inhibiting SCF^{TrCP} on EMI1 stability. We predicted that SCF^{TrCP} inhibition may stabilize EMI1 in HFF C while having less of an effect in HFF E7 if SCF^{TrCP} activity was already inhibited. HFF C and HFF E7 were arrested at the G1/S boundary with a double thymidine block and then released into nocodazole. At 7.5 hours after release into nocodazole, 1 μM MLN4924 or DMSO was added. MLN4924 is a small molecule inhibitor of the NEDD8-activating enzyme (NAE) (Soucy et al., 2009), which is an essential enzyme in the first step of NEDD8 conjugation. Since NEDD8 conjugation to cullins is required for activation of ubiquitin ligase activity of cullin RING ligases including SCF^{TrCP} (Duda et al., 2008; Podust et al., 2000; Read et al., 2000), MLN4924 treatment will cause accumulation of SCF^{TrCP} substrates. Cells were harvested at 0.5, 2.5, 4.5, and 6.5 hours after MLN4924/DMSO treatment, corresponding to 8, 10, 12, and 14 hours after release into nocodazole. The disappearance of NEDD8-conjugated CUL1 (indicated by an asterisk, Fig 4A) illustrated the effectiveness of the inhibitor. MLN4924 treatment decreased the mitotic cell population indicated by assessment of the mitotic markers the slower migrating phosphorylated form of CDC27 and H3-pS10 as well as FACS analyses (Fig 4A). This is likely due to accumulation of some inhibitor of mitotic entry that is normally degraded after ubiquitylation by cullin RING ligases. Nonetheless, cyclin A degradation still occurred in MLN4924 treated HFF C populations (Fig 4). Interestingly, the decrease of EMI1 levels in MLN4924 treated HFF C

was markedly inhibited (29%) as compared to DMSO treated HFF C (100%). In contrast the stabilization of EMI1 by MLN4924 treatment was minimal in HFF E7 (0% decrease as compared to 19% in DMSO treated HFF E7). Likewise, MLN4924 treatment stabilized WEE1A more effectively in HFF C than in HFF E7, even though WEE1A was not as stable as EMI1 in HFF E7. No decrease of WEE1A levels was observed in MLN4924 as compared to 72% in DMSO treated HFF C and no decrease was observed in MLN4924 as compared to 37% in DMSO treated HFF E7. Taken together, these results support our hypothesis that HPV16 E7 expression inhibits SCF^{TrCP}-mediated EMI1 ubiquitylation and subsequent proteasomal degradation during mitosis.

EMI1 depletion partially restores cyclin A and NEK2A degradation in HPV16 E7-expressing cells

In order to determine whether HPV16 E7 expression may inhibit cyclin A and NEK2A degradation by upregulating mitotic EMI1 levels, we transfected HFF C and HFF E7 with EMI1 targeting siRNA pools, arrested the cells at the G1/S boundary by a double thymidine block followed by release into nocodazole. EMI1 protein levels were reduced after siRNA transfection, but we consistently detected higher residual EMI1 levels in HFF E7 than in HFF C (Fig 5A and data not shown). In HFF E7, EMI1 depletion caused a 26% decrease in cyclin A levels as compared to no decrease in HFF E7 transfected with control siRNAs. Similarly, EMI1 depletion in HFF E7 caused a 47% decrease in NEK2A levels as compared to no decrease in HFF E7 transfected with control siRNAs (Fig 5A and 5B). Cyclin B and securin levels were not quantified since both remained stable in the nocodazole-arrested cells. Although EMI1 depletion in HFF E7 did not fully restore cyclin A and NEK2A degradation to the levels observed in HFF C populations, the results further strengthen our model that EMI1 accumulation contributes to the inhibition of APC/C substrate degradation in E7-expressing cells.

DISCUSSION

We have previously shown that HPV16 E7 expression impedes the degradation of cyclins A and B during mitosis at least in part by engaging the SAC (Yu and Munger, 2012). Cyclins A and B degradation is triggered by APC/C mediated ubiquitylation. APC/C dysfunction and overexpression of APC/C substrates has been detected in many cancers and has been referred to as a “mitotic profile” (Carter et al., 2006; Lehman et al., 2007). Hence we set out to investigate whether HPV16 E7 oncoprotein expression may cause defects in APC/C activity as well. Here we report that in addition to cyclins A and B, mitotic steady state levels of other APC/C substrates including NEK2A, securin, CDC20, PLK1 and Aurora B were also increased in E7-expressing cells (Fig 1). Since cyclin A and NEK2A degradation is not regulated by the SAC (van Zon and Wolthuis, 2010), our results are consistent with the model that E7 may inhibit APC/C activity in an SAC-independent manner.

We initially examined the SAC-independent APC/C inhibitor EMI1. EMI1 expression is controlled by E2F and given that HPV16 E7 dysregulates E2F activity by degrading pRB family members (Hsu et al., 2002; Huh et al., 2007), it is not surprising that EMI1 mRNA levels were higher in HFF E7 than in HFF C populations (Fig 2C). The most striking differences in EMI1 protein levels between HFF E7 and HFF C populations were detected during mitosis, when EMI1 is normally degraded due to SCF^{TrCP}-mediated ubiquitylation (Hansen et al., 2004; Margottin-Goguet et al., 2003). The resulting doubling of the EMI1 half-life from ~1 hour to ~2 hours (Fig 3B) may have major consequences during mitosis, which usually lasts only about ~1 hour. The finding that treatment with MLN4924, which inactivates cullin RING ligases including SCF^{TrCP}, renders mitotic EMI1 levels consistently high in HFF C while having less additional effects on the consistently high EMI1 levels in

HFF E7 populations (Fig 4), is consistent with the model that SCF^{TrCP}-mediated EMI1 ubiquitylation is already inhibited in HFF E7 populations.

The mechanism by which HPV16 E7 may inhibit SCF^{TrCP}-mediated EMI1 ubiquitylation remains unknown. It has been reported that HPV16 E7 can associate with the SCF^{TrCP} scaffold component CUL1 (Oh et al., 2004) and this may account for the observed inhibition of EMI1 degradation during mitosis. Our own co-immunoprecipitation experiments in HFF E7 and other HPV16 E7-expressing cells, however, did not confirm such an interaction (data not shown). We also did not observe higher levels of E7 or pRB upon MLN4924 treatment (Fig 4A), even though they have both been reported to be substrates of cullin RING ligases (Huh et al., 2007; Oh et al., 2004). In the case of pRB, it is conceivable that the relatively long half-life of pRB in E7 expressing cells (~3 hours) will preclude the marked accumulation of the protein upon MLN4924 treatment for time investigated in this experiment (Boyer et al., 1996; Gonzalez et al., 2001).

E7 may also inhibit EMI1 degradation by affecting EMI1 phosphorylation by CDK1 and PLK1, which is required for SCF^{TrCP}-mediated EMI1 ubiquitylation (Hansen et al., 2004; Hsu et al., 2002; Margottin-Goguet et al., 2003; Moshe et al., 2004). Our results show that E7 expression does not generally inhibit PLK1 activity as assessed by PLK1 phosphorylation of cyclin B at serine 133 (Fig 2A). We cannot rule out, however, that E7 may specifically interfere with PLK1 phosphorylation of EMI1, or that E7 may inhibit CDK1 phosphorylation of EMI1, which stimulates EMI1 ubiquitylation by SCF^{TrCP} synergistically with PLK1 phosphorylation (Moshe et al., 2004). Alternatively, E7 may generally inhibit SCF^{TrCP} activity. To address this possibility, we examined the classical SCF^{TrCP} substrate β-catenin. We did not detect marked alterations in β-catenin protein levels either in the synchronization or the cycloheximide chase experiments (data not shown). Possible interpretations are that β-catenin has a long half-life and Axin and/or other cofactors may be required to accelerate the degradation (Kitagawa et al., 1999), or that β-catenin is not degraded in a similar cell cycle-regulated manner as EMI1 and WEE1A. Concerning WEE1A, our experiments failed to provide conclusive data as to whether it may be stabilized in HFF E7 populations. On the one hand, Wee1A levels did not decrease as much in HFF E7 as in HFF C populations during mitosis (Fig 2). On the other hand there was no marked difference when WEE1A half-lives were compared in HFF E7 and HFF C populations by cycloheximide chase experiments similar to the one in Fig 3 by examining even longer time frame (data not shown). The observed accumulation of WEE1A protein in HFF E7 may, therefore represent a secondary effect to the buildup of EMI1, which competes with WEE1A for access to SCF^{TrCP}. While our results do not rule out the possibility that E7 may generally inhibit SCF^{TrCP} activity, this appears unlikely since it has been reported that SCF^{TrCP}-mediated claspin turnover during recovery from DNA damage checkpoint is accelerated in HPV16 E7-expressing cells (Spardy et al., 2009). Thus, E7 appears to differentially affect individual SCF^{TrCP} substrates that are degraded during mitosis or recovery from DNA damage checkpoint in G2 phase.

Given our finding that mitotic HFF E7 populations contain higher steady state levels of the APC/C inhibitor EMI1 than control cells, we next investigated whether this may contribute to the inhibition of APC/C substrate degradation that we observed in HPV16 E7-expressing cells. Consistent with this model, degradation of cyclin A and NEK2A was partially restored by depleting EMI1 in HFF E7. The observed incomplete restoration of cyclin A and NEK2A degradation in HFF E7 populations may be due to residual detectable EMI1 in HFF E7 populations that persisted throughout the course of the experiment (Fig 5).

Inhibition of SCF^{TrCP} with MLN4924 in HFF C populations caused increased mitotic EMI1 levels similar to those present in HFF E7 populations (Fig 4). Interestingly, however, we did

not observe inhibition of cyclin A degradation in MLN4924 treated HFF C as in HFF E7 populations (Fig 4). This appears inconsistent with our model that inhibition of SCF^{TrCP}-mediated EMI1 degradation may account for the observed inhibition of cyclin A degradation in HFF E7 populations. There are some caveats to this experiment, however. While SCF^{TrCP} inhibition by MLN4924 clearly causes increased levels of EMI1, they may not be fully active in inhibiting APC/C as the EMI1 activity can be regulated at the level of subcellular localization or by phosphorylation (Moshe et al., 2011).

Although it is generally accepted that EMI1 inhibits the interphase APC/C^{CDH1} complex, there remains some controversy over whether EMI1 is essential for the inhibition of the mitotic APC/C^{CDC20} complex. On the one hand, ectopic expression of a non-destructible EMI1 results in a prometaphase delay and causes varying degrees of stabilization of cyclin A and NEK2A, as well as of APC/C^{CDH1} substrates such as Aurora A, similar to what we have detected in HPV16 E7-expressing cells (Margottin-Goguet et al., 2003). Moreover, experiments with $TrCP1^{-/-}$ mouse embryo fibroblasts revealed that EMI1 stabilization during mitosis is correlated with a delayed mitotic progression and inhibition of cyclins A and B degradation (Guardavaccaro et al., 2003). On the other hand, live cell imaging experiments showed that PLK1 inhibition by RNA interference or with a small molecule PLK1 inhibitor did not affect cyclin A degradation despite marked stabilization of EMI1 (Kraft et al., 2003; Lenart et al., 2007; van Vugt et al., 2004). The discrepancies in the literature may be due to different levels of EMI1 overexpression. Importantly, HFF E7 had significantly more EMI1 during mitosis, over 10 fold more at 12 and 14 hours after release into nocodazole than in HFF C (Fig 2, quantification not shown), consistent with our model that dysregulation of EMI1 by HPV16 E7 may inhibit APC/C activity and delay mitotic progression.

There are several important implications from our findings that HPV16 E7 affects APC/C function and dysregulates EMI1 expression at the levels of both transcription and protein stability. Firstly, overexpression of EMI1 is oncogenic in p53-deficient cells (Lehman et al., 2006), which is especially relevant in high-risk HPV-associated cancers where p53 is degraded due to E6 expression. Furthermore, overexpression of APC/C substrates including cyclin B, securin, Aurora kinases, PLK1, and SKP2, individually, has been implicated in genomic instability and cancer development (Lehman et al., 2007). As a result, the overexpression of EMI1 and the resulting accumulation of APC/C substrates may contribute to E7's transforming activities.

Secondly, dysregulation of EMI1 may importantly contribute to the mitotic abnormalities in HPV16 E7-expressing cells. The overexpression of EMI1 and HPV16 E7 results in similar mitotic phenotypes including a prometaphase delay and centrosome overduplication (Duensing et al., 2000; Duensing and Munger, 2002; Guardavaccaro et al., 2003; Margottin-Goguet et al., 2003; Nguyen and Munger, 2009). Accumulation of the mitotic regulators including cyclin A (Balczon, 2001), NEK2A (Hayward et al., 2004), PLK1 (Mundt et al., 1997), and Aurora A (Meraldi et al., 2002), can clearly contribute to mitotic abnormalities including centrosome overduplication. Moreover, HPV16 E7 and EMI1 both localize to centrosomes and have been reported to associate with nuclear mitotic apparatus protein 1 (NuMA) individually (Ban et al., 2007; Nguyen et al., 2007; Nguyen and Munger, 2009). Although we did not find association between E7 and EMI1 by co-immunoprecipitations, it is conceivable that the functional interplay between E7 and EMI1 may also cause inhibition of APC/C at centrosomes.

Lastly, inhibition of APC/C by HPV16 E7 may have implications for the viral life cycle. Many viruses seem to subvert APC/C activity (Fehr and Yu, 2013; Heilman et al., 2005; Mo et al., 2012). Since ribonucleotide reductase subunit 2 (R2), thymidine kinase 1 (TK) and

thymidylate kinase (TMPK) are APC/C^{CDH1} substrates and required for DNA replication, it has been suggested APC/C inhibition creates a permissive environment for DNA replication of viruses that otherwise do not express these DNA replication factors (Mo et al., 2012). Although it is currently unclear what roles the inhibition of APC/C may play in the HPV viral life cycle, it is worth investigating given that high-risk HPV E2, a viral replication and transcription factor, whose expression is often lost during carcinogenesis, also inhibits the APC/C by binding to the co-activators CDC20 and CDH1 (Bellanger et al., 2005).

In summary, we report that HPV16 E7 inhibits APC/C substrate degradation and that the dysregulation of EMI1 expression at both the transcription and protein stability levels may contribute to the mitotic delay and inhibition of APC/C substrate degradation in HPV16 E7-expressing cells. In the future it will be interesting to further elucidate the functional interplay between EMI1 and HPV16 E7 beyond mitosis and to determine whether there are other mechanisms by which HPV oncoproteins may dysregulate APC/C activity.

MATERIALS AND METHODS

Cells

Primary human foreskin fibroblasts (HFFs) and human foreskin keratinocytes (HFKs) were isolated from anonymous newborn circumcisions as previously described (McLaughlin-Drubin et al., 2008). HFFs with stable expression of HPV16 E7 were generated by infecting primary HFF populations with pBABE-puromycin-based retroviral vectors and selected with 1μg/ml puromycin. Recombinant retroviruses were produced in 293T cells as previously described (Piboonniyom et al., 2003). Infections of 50% confluent HFFs were performed with a mixture of 2 ml viral supernatant, 8 μg/ml Polybrene, and 2 ml Dulbecco's modified Eagle medium (DMEM) for 4–6 hours. HFFs were maintained in DMEM supplemented with 10% fetal bovine serum, 50 U/ml penicillin and 50 μg/ml streptomycin. HFKs with stable expression of HPV16 E7 were generated by retroviral infection with pLXSN based vectors and maintained in keratinocytes serum-free medium (KSFM) supplemented with human recombinant epidermal growth factor 1–53, bovine pituitary extract (Invitrogen), 50 U/ml penicillin and 50 μg/ml streptomycin, 20 μg/ml gentamicin, and 1 μg/ml amphotericin B. All experiments were performed with HFF or HFK populations passaged less than ten times.

Western Blotting and Antibodies

Cells were lysed in ML buffer (300 mM NaCl, 0.5% Nonidet P-40 [NP-40], 20 mM Tris-HCl [pH 8.0], 1 mM EDTA) supplemented with one complete EDTA-free protease inhibitor cocktail tablet (Roche) per 25 ml lysis buffer and one PhosSTOP phosphatase inhibitor cocktail tablet (Roche) per 10 ml lysis buffer. Lysates were cleared by centrifugation at 16,000 × g for 15 min at 4°C. Protein concentrations were determined by Bradford assay (Bio-Rad). 20 to 40 μg total protein was separated by 4–12% NuPAGE® Bis-Tris precast gels (Invitrogen) and electro transferred onto polyvinylidenedifluoride (PVDF) membranes (Immobilon-P; Millipore). Larger amount of total protein (100 to 200 μg) was separated by self-cast 12% SDS PAGE gels and electro transferred to PVDF membranes as well. Membranes were blocked in 5% nonfat dry milk in TNET buffer (200 mM Tris-HCl, 1 M NaCl, 50 mM EDTA, 0.1% Tween 20 [pH 7.5]) or 5% BSA in TBST (137 mM NaCl, 2.7 mM KCl, 25 mM Tris [pH 7.4], 0.1% Tween 20) and probed with appropriate antibodies. The following primary antibodies were used at the indicated dilutions: pRB (AB-5, CalBiochem, 1:100), cyclin A (sc-751, Santa Cruz Biotechnology, 1:500), NEK2A (610593, BD Transduction Laboratories, 1:1000), cyclin B (610219, BD Transduction Laboratories, 1:1,000), securin (ab3305, Abcam, 1:500), CDC20 (sc-8358, Santa Cruz Biotechnology, 1:200), PLK1 (33–1700, Invitrogen, 1:500), Aurora B (ab2254, Abcam, 1:1000), CDC27

(610454, BD Transduction Laboratories, 1:1000), H3-pS10 (ab5176, Abcam, 1:500), EMI1 (37–6600, Invitrogen, 1:100), WEE1A (sc-5285, Santa Cruz Biotechnology, 1:200), cyclin B-pS133 (4133, Cell Signaling, 1:1000), CUL1 (71–8700, Invitrogen, 1:500), and actin (MAB1501, Millipore, 1:1,000). Secondary anti-mouse and anti-rabbit antibodies conjugated to horseradish peroxidase were used at a 1:10,000 dilution. Proteins were visualized by enhanced chemiluminescence (Perkin Elmer, Millipore) and exposed on Kodak BioMax XAR film, or electronically acquired with a molecular imaging system (Carestream, GL 4000 Pro). Band intensities of Western blots were quantified with ImageJ.

Cell Synchronization and RNAi

HFFs were synchronized by a double thymidine block by treating cells with 2 mM thymidine for 18 hours, followed by an 8 hour release in normal medium and treatment with 2 mM thymidine for an additional 17 hours. Then cells were released into normal medium or in medium containing 100 ng/ml nocodazole (Sigma). For siRNA transfection, 2×10^5 HFF cells were seeded in 6 cm plates one day before transfection with 200 pmol EMI1-specific ON-TARGETplusSMARTpool (L-012434-00-0005; Thermo Scientific Dharmacon) or ON-TARGETplus Non-Targeting Pool (D-001810-10-05; Thermo Scientific Dharmacon) using Lipofectamine 2000 (Invitrogen). At one day after siRNA transfection, HFFs were subjected to a double thymidine block and released into nocodazole before being harvested for Western blot analyses.

Flow Cytometry

To measure mitotic indices, cells were fixed with 70% ice-cold ethanol, rinsed with 1% fetal bovine serum in phosphate buffered saline (PBS), stained for MPM-2 (05-368, Upstate/Millipore, 1:1,000) for one hour at room temperature, and with Alexa Fluor® 488 Goat Anti-Mouse IgG (H+L) (Molecular Probes/Invitrogen, 1:400) for one hour at room temperature in the dark followed by staining with propidium iodide (Sigma, 30 μg/ml in PBS) for 30 minutes in the dark. Flow cytometry was conducted on FACSCalibur (Becton Dickinson, Franklin Lakes, NJ). Data were acquired using the CellQuest software (Becton Dickinson) and analyzed with FlowJo 7.6.5.

Immunofluorescence

HFFs were seeded on coverslips in 12-well plates at least one day before and then fixed with 4% formaldehyde in PBS. After permeabilization with 0.5% Triton X-100 in PBS, they were blocked with 5% BSA in PBS. Ki67 staining was performed by incubation with the primary antibody (ab15580, Abcam, 1:100) followed by Alexa Fluor® 488 Goat Anti-Rabbit IgG (H+L) (Molecular Probes/Invitrogen, 1:1000). Coverslips were mounted with ProLong® Gold Antifade Reagent with DAPI (Life Technologies). Images were taken by an Axioplan 2 microscope (Zeiss) and acquired with Axiovision 4.5 software (Zeiss).

qRT-PCR

Lysates from 3 biological triplicates were prepared and qRT-PCR was performed using the TaqMan® Reverse Transcription Reagents (Applied Biosystems) followed by amplification with the Fast SYBR® Green Master Mix (Applied Biosystems) according to manufacturer's instructions. Primers used were EMI1 (HP210168, OriGene Technologies) and GAPDH (HP205798, OriGene Technologies). Analysis was performed using a StepOnePlus Real-Time PCR System (Applied Biosystems).

Cycloheximide Chase

To determine EMI1 half-life, HFFs were arrested in mitosis with 100 ng/ml nocodazole for 18 hours, and 25 μg/ml cycloheximide (Enzo Life Sciences) was added to the medium. Cells

were harvested at every 30 minutes as indicated, for up to 2 hours after cycloheximide addition.

Acknowledgments

We thank Drs. James DeCaprio, Jonathan Higgins, and Jagesh Shah for constructive advice, Dr. David Knipe and his lab for sharing the microscope, Tyshia Gwin, Mallory Harden, and Margaret McLaughlin-Drubin for kindly sharing HFK populations, and all the other Munger laboratory members for helpful discussions and technical assistance. This work was supported by PHS Grants R01 CA066980 and R01 CA081135.

REFERENCES

Balczon RC. Overexpression of cyclin A in human HeLa cells induces detachment of kinetochores and spindle pole/centrosome overproduction. Chromosoma. 2001; 110:381–392. [PubMed: 11734996]

Ban KH, Torres JZ, Miller JJ, Mikhailov A, Nachury MV, Tung JJ, Rieder CL, Jackson PK. The END network couples spindle pole assembly to inhibition of the anaphase-promoting complex/cyclosome in early mitosis. Developmental cell. 2007; 13:29–42. [PubMed: 17609108]

Bellanger S, Blachon S, Mechali F, Bonne-Andrea C, Thierry F. High-risk but not low-risk HPV E2 proteins bind to the APC activators Cdh1 and Cdc20 and cause genomic instability. Cell Cycle. 2005; 4:1608–1615. [PubMed: 16222116]

Boyer SN, Wazer DE, Band V. E7 protein of human papilloma virus-16 induces degradation of retinoblastoma protein through the ubiquitin-proteasome pathway. Cancer Res. 1996; 56:4620–4624. [PubMed: 8840974]

Carter SL, Eklund AC, Kohane IS, Harris LN, Szallasi Z. A signature of chromosomal instability inferred from gene expression profiles predicts clinical outcome in multiple human cancers. Nature genetics. 2006; 38:1043–1048. [PubMed: 16921376]

Di Fiore B, Pines J. Emi1 is needed to couple DNA replication with mitosis but does not regulate activation of the mitotic APC/C. The Journal of cell biology. 2007; 177:425–437. [PubMed: 17485488]

Duda DM, Borg LA, Scott DC, Hunt HW, Hammel M, Schulman BA. Structural insights into NEDD8 activation of cullin-RING ligases: conformational control of conjugation. Cell. 2008; 134:995–1006. [PubMed: 18805092]

Duensing S, Lee LY, Duensing A, Basile J, Piboonniyom S, Gonzalez S, Crum CP, Munger K. The human papillomavirus type 16 E6 and E7 oncoproteins cooperate to induce mitotic defects and genomic instability by uncoupling centrosome duplication from the cell division cycle. Proceedings of the National Academy of Sciences of the United States of America. 2000; 97:10002–10007. [PubMed: 10944189]

Duensing S, Munger K. The human papillomavirus type 16 E6 and E7 oncoproteins independently induce numerical and structural chromosome instability. Cancer Res. 2002; 62:7075–7082. [PubMed: 12460929]

Engelbert D, Schnerch D, Baumgarten A, Wasch R. The ubiquitin ligase APC(Cdh1) is required to maintain genome integrity in primary human cells. Oncogene. 2008; 27:907–917. [PubMed: 17700535]

Fehr AR, Yu D. Control the host cell cycle: viral regulation of the anaphase-promoting complex. Journal of virology. 2013; 87:8818–8825. [PubMed: 23760246]

Frye JJ, Brown NG, Petzold G, Watson ER, Grace CR, Nourse A, Jarvis MA, Kriwacki RW, Peters JM, Stark H, Schulman BA. Electron microscopy structure of human APC/C-EMI1 reveals multimodal mechanism of E3 ligase shutdown. Nature structural & molecular biology. 2013

Garcia-Higuera I, Manchado E, Dubus P, Canamero M, Mendez J, Moreno S, Malumbres M. Genomic stability and tumour suppression by the APC/C cofactor Cdh1. Nature cell biology. 2008; 10:802–811.

Gonzalez SL, Stremlau M, He X, Basile JR, Munger K. Degradation of the retinoblastoma tumor suppressor by the human papillo-mavirus type 16 E7 oncoprotein is important for functional inactivation and is separable from proteasomal degradation of E7. Journal of virology. 2001; 75:7583–7591. [PubMed: 11462030]

Guardavaccaro D, Kudo Y, Boulaire J, Barchi M, Busino L, Donzelli M, Margottin-Goguet F, Jackson PK, Yamasaki L, Pagano M. Control of meiotic and mitotic progression by the F box protein beta-Trcp1 in vivo. Developmental cell. 2003; 4:799–812. [PubMed: 12791266]

Hansen DV, Loktev AV, Ban KH, Jackson PK. Plk1 regulates activation of the anaphase promoting complex by phosphorylating and triggering SCFbetaTrCP-dependent destruction of the APC Inhibitor Emi1. Molecular biology of the cell. 2004; 15:5623–5634. [PubMed: 15469984]

Hayward DG, Clarke RB, Faragher AJ, Pillai MR, Hagan IM, Fry AM. The centrosomal kinase Nek2 displays elevated levels of protein expression in human breast cancer. Cancer Res. 2004; 64:7370–7376. [PubMed: 15492258]

Heilman DW, Green MR, Teodoro JG. The anaphase promoting complex: a critical target for viral proteins and anti-cancer drugs. Cell Cycle. 2005; 4:560–563. [PubMed: 15876865]

Hsu JY, Reimann JD, Sorensen CS, Lukas J, Jackson PK. E2F-dependent accumulation of hEmi1 regulates S phase entry by inhibiting APC(Cdh1). Nature cell biology. 2002; 4:358–366.

Huh K, Zhou X, Hayakawa H, Cho JY, Libermann TA, Jin J, Harper JW, Munger K. Human papillomavirus type 16 E7 oncoprotein associates with the cullin 2 ubiquitin ligase complex, which contributes to degradation of the retinoblastoma tumor suppressor. Journal of virology. 2007; 81:9737–9747. [PubMed: 17609271]

Jackman M, Lindon C, Nigg EA, Pines J. Active cyclin B1-Cdk1 first appears on centrosomes in prophase. Nature cell biology. 2003; 5:143–148.

Jeganathan KB, Malureanu L, van Deursen JM. The Rae1-Nup98 complex prevents aneuploidy by inhibiting securin degradation. Nature. 2005; 438:1036–1039. [PubMed: 16355229]

Kitagawa M, Hatakeyama S, Shirane M, Matsumoto M, Ishida N, Hattori K, Nakamichi I, Kikuchi A, Nakayama K. An F-box protein, FWD1, mediates ubiquitin-dependent proteolysis of beta-catenin. The EMBO journal. 1999; 18:2401–2410. [PubMed: 10228155]

Klingelhutz AJ, Roman A. Cellular transformation by human papillomaviruses: lessons learned by comparing high- and low-risk viruses. Virology. 2012; 424:77–98. [PubMed: 22284986]

Kraft C, Herzog F, Gieffers C, Mechtler K, Hagting A, Pines J, Peters JM. Mitotic regulation of the human anaphase-promoting complex by phosphorylation. The EMBO journal. 2003; 22:6598–6609. [PubMed: 14657031]

Lehman NL, Tibshirani R, Hsu JY, Natkunam Y, Harris BT, West RB, Masek MA, Montgomery K, van de Rijn M, Jackson PK. Oncogenic regulators and substrates of the anaphase promoting complex/cyclosome are frequently overexpressed in malignant tumors. The American journal of pathology. 2007; 170:1793–1805. [PubMed: 17456782]

Lehman NL, Verschuren EW, Hsu JY, Cherry AM, Jackson PK. Overexpression of the anaphase promoting complex/cyclosome inhibitor Emi1 leads to tetraploidy and genomic instability of p53-deficient cells. Cell Cycle. 2006; 5:1569–1573. [PubMed: 16861914]

Lenart P, Petronczki M, Steegmaier M, Di Fiore B, Lipp JJ, Hoffmann M, Rettig WJ, Kraut N, Peters JM. The small-molecule inhibitor BI 2536 reveals novel insights into mitotic roles of polo-like kinase 1. Current biology : CB. 2007; 17:304–315. [PubMed: 17291761]

Lipkowitz S, Weissman AM. RINGs of good and evil: RING finger ubiquitin ligases at the crossroads of tumour suppression and oncogenesis. Nature reviews. Cancer. 2011; 11:629–643.

Margottin-Goguet F, Hsu JY, Loktev A, Hsieh HM, Reimann JD, Jackson PK. Prophase destruction of Emi1 by the SCF(betaTrCP/Slimb) ubiquitin ligase activates the anaphase promoting complex to allow progression beyond prometaphase. Developmental cell. 2003; 4:813–826. [PubMed: 12791267]

McLaughlin-Drubin ME, Huh KW, Munger K. Human papillomavirus type 16 E7 oncoprotein associates with E2F6. J Virol. 2008; 82:8695–8705. [PubMed: 18579589]

McLaughlin-Drubin ME, Meyers J, Munger K. Cancer associated human papillomaviruses. Current opinion in virology. 2012; 2:459–466. [PubMed: 22658985]

McLaughlin-Drubin ME, Munger K. The human papillomavirus E7 oncoprotein. Virology. 2009a; 384:335–344. [PubMed: 19007963]

McLaughlin-Drubin ME, Munger K. Oncogenic activities of human papillomaviruses. Virus Res. 2009b; 143:195–208. [PubMed: 19540281]

Meraldi P, Honda R, Nigg EA. Aurora-A overexpression reveals tetraploidization as a major route to centrosome amplification in p53−/− cells. The EMBO journal. 2002; 21:483–492. [PubMed: 11847097]

Miller JJ, Summers MK, Hansen DV, Nachury MV, Lehman NL, Loktev A, Jackson PK. Emi1 stably binds and inhibits the anaphase-promoting complex/cyclosome as a pseudosubstrate inhibitor. Genes & development. 2006; 20:2410–2420. [PubMed: 16921029]

Mo M, Shahar S, Fleming SB, Mercer AA. How viruses affect the cell cycle through manipulation of the APC/C. Trends in microbiology. 2012

Moody CA, Laimins LA. Human papillomavirus oncoproteins: pathways to transformation. Nature reviews. Cancer. 2010; 10:550–560.

Moshe Y, Bar-On O, Ganoth D, Hershko A. Regulation of the action of early mitotic inhibitor 1 on the anaphase-promoting complex/cyclosome by cyclin-dependent kinases. The Journal of biological chemistry. 2011; 286:16647–16657. [PubMed: 21454540]

Moshe Y, Boulaire J, Pagano M, Hershko A. Role of Polo-like kinase in the degradation of early mitotic inhibitor 1, a regulator of the anaphase promoting complex/cyclosome. Proceedings of the National Academy of Sciences of the United States of America. 2004; 101:7937–7942. [PubMed: 15148369]

Mundt KE, Golsteyn RM, Lane HA, Nigg EA. On the regulation and function of human polo-like kinase 1 (PLK1): effects of overexpression on cell cycle progression. Biochemical and biophysical research communications. 1997; 239:377–385. [PubMed: 9344838]

Munger K, Baldwin A, Edwards KM, Hayakawa H, Nguyen CL, Owens M, Grace M, Huh K. Mechanisms of human papillomavirus-induced oncogenesis. Journal of virology. 2004; 78:11451–11460. [PubMed: 15479788]

Musacchio A, Salmon ED. The spindle-assembly checkpoint in space and time. Nature reviews. Molecular cell biology. 2007; 8:379–393.

Nakayama KI, Nakayama K. Regulation of the cell cycle by SCF-type ubiquitin ligases. Seminars in cell & developmental biology. 2005; 16:323–333. [PubMed: 15840441]

Nakayama KI, Nakayama K. Ubiquitin ligases: cell-cycle control and cancer. Nature reviews. Cancer. 2006; 6:369–381.

Nguyen CL, Eichwald C, Nibert ML, Munger K. Human papillomavirus type 16 E7 oncoprotein associates with the centrosomal component gamma-tubulin. Journal of virology. 2007; 81:13533–13543. [PubMed: 17913829]

Nguyen CL, Munger K. Human papillomavirus E7 protein deregulates mitosis via an association with nuclear mitotic apparatus protein 1. Journal of virology. 2009; 83:1700–1707. [PubMed: 19052088]

Oh KJ, Kalinina A, Wang J, Nakayama K, Nakayama KI, Bagchi S. The papillomavirus E7 oncoprotein is ubiquitinated by UbcH7 and Cullin 1- and Skp2-containing E3 ligase. Journal of virology. 2004; 78:5338–5346. [PubMed: 15113913]

Peters JM. The anaphase promoting complex/cyclosome: a machine designed to destroy. Nature reviews. Molecular cell biology. 2006; 7:644–656.

Piboonniyom SO, Duensing S, Swilling NW, Hasskarl J, Hinds PW, Munger K. Abrogation of the retinoblastoma tumor suppressor checkpoint during keratinocyte immortalization is not sufficient for induction of centrosome-mediated genomic instability. Cancer Res. 2003; 63:476–483. [PubMed: 12543805]

Pines J. Cubism and the cell cycle: the many faces of the APC/C. Nature reviews. Molecular cell biology. 2011; 12:427–438.

Podust VN, Brownell JE, Gladysheva TB, Luo RS, Wang C, Coggins MB, Pierce JW, Lightcap ES, Chau V. A Nedd8 conjugation pathway is essential for proteolytic targeting of p27Kip1 by ubiquitination. Proceedings of the National Academy of Sciences of the United States of America. 2000; 97:4579–4584. [PubMed: 10781063]

Read MA, Brownell JE, Gladysheva TB, Hottelet M, Parent LA, Coggins MB, Pierce JW, Podust VN, Luo RS, Chau V, Palombella VJ. Nedd8 modification of cul-1 activates SCF(beta(TrCP))-dependent ubiquitination of IkappaBalpha. Molecular and cellular biology. 2000; 20:2326–2333. [PubMed: 10713156]

Reimann JD, Freed E, Hsu JY, Kramer ER, Peters JM, Jackson PK. Emi1 is a mitotic regulator that interacts with Cdc20 and inhibits the anaphase promoting complex. Cell. 2001a; 105:645–655. [PubMed: 11389834]

Reimann JD, Gardner BE, Margottin-Goguet F, Jackson PK. Emi1 regulates the anaphase-promoting complex by a different mechanism than Mad2 proteins. Genes & development. 2001b; 15:3278–3285. [PubMed: 11751633]

Scheffner M, Huibregtse JM, Vierstra RD, Howley PM. The HPV-16 E6 and E6-AP complex functions as a ubiquitin-protein ligase in the ubiquitination of p53. Cell. 1993; 75:495–505. [PubMed: 8221889]

Song MS, Song SJ, Ayad NG, Chang JS, Lee JH, Hong HK, Lee H, Choi N, Kim J, Kim H, Kim JW, Choi EJ, Kirschner MW, Lim DS. The tumour suppressor RASSF1A regulates mitosis by inhibiting the APC-Cdc20 complex. Nature cell biology. 2004; 6:129–137.

Soucy TA, Smith PG, Milhollen MA, Berger AJ, Gavin JM, Adhikari S, Brownell JE, Burke KE, Cardin DP, Critchley S, Cullis CA, Doucette A, Garnsey JJ, Gaulin JL, Gershman RE, Lublinsky AR, McDonald A, Mizutani H, Narayanan U, Olhava EJ, Peluso S, Rezaei M, Sintchak MD, Talreja T, Thomas MP, Traore T, Vyskocil S, Weatherhead GS, Yu J, Zhang J, Dick LR, Claiborne CF, Rolfe M, Bolen JB, Langston SP. An inhibitor of NEDD8-activating enzyme as a new approach to treat cancer. Nature. 2009; 458:732–736. [PubMed: 19360080]

Spardy N, Covella K, Cha E, Hoskins EE, Wells SI, Duensing A, Duensing S. Human papillomavirus 16 E7 oncoprotein attenuates DNA damage checkpoint control by increasing the proteolytic turnover of claspin. Cancer Res. 2009; 69:7022–7029. [PubMed: 19706760]

Suijkerbuijk SJ, Kops GJ. Preventing aneuploidy: the contribution of mitotic checkpoint proteins. Biochim Biophys Acta. 2008; 1786:24–31. [PubMed: 18472014]

van Vugt MA, van de Weerdt BC, Vader G, Janssen H, Calafat J, Klompmaker R, Wolthuis RM, Medema RH. Polo-like kinase-1 is required for bipolar spindle formation but is dispensable for anaphase promoting complex/Cdc20 activation and initiation of cytokinesis. The Journal of biological chemistry. 2004; 279:36841–36854. [PubMed: 15210710]

van Zon W, Wolthuis RM. Cyclin A and Nek2A: APC/C-Cdc20 substrates invisible to the mitotic spindle checkpoint. Biochemical Society transactions. 2010; 38:72–77. [PubMed: 20074038]

Wang W, Kirschner MW. Emi1 preferentially inhibits ubiquitin chain elongation by the anaphase-promoting complex. Nature cell biology. 2013

Watanabe N, Arai H, Iwasaki J, Shiina M, Ogata K, Hunter T, Osada H. Cyclin-dependent kinase (CDK) phosphorylation destabilizes somatic Wee1 via multiple pathways. Proceedings of the National Academy of Sciences of the United States of America. 2005; 102:11663–11668. [PubMed: 16085715]

White EA, Sowa ME, Tan MJ, Jeudy S, Hayes SD, Santha S, Munger K, Harper JW, Howley PM. Systematic identification of interactions between host cell proteins and E7 oncoproteins from diverse human papillomaviruses. Proceedings of the National Academy of Sciences of the United States of America. 2012; 109:E260–E267. [PubMed: 22232672]

Winkler B, Crum CP, Fujii T, Ferenczy A, Boon M, Braun L, Lancaster WD, Richart RM. Koilocytotic lesions of the cervix. The relationship of mitotic abnormalities to the presence of papillomavirus antigens and nuclear DNA content. Cancer. 1984; 53:1081–1087. [PubMed: 6318958]

Yu Y, Munger K. Human papillomavirus type 16 E7 oncoprotein engages but does not abrogate the mitotic spindle assembly checkpoint. Virology. 2012; 432:120–126. [PubMed: 22748180]

HIGHLIGHTS

- HPV16 E7 inhibits degradation of a wide range of APC/C substrates during mitosis.
- We study how E7 inhibits cyclin A and NEK2A degradation independent of the SAC.
- Mitotic levels of EMI1, an APC/C inhibitor, are significantly upregulated by E7.
- Dysregulation of EMI1 by E7 occurs at mRNA and protein stability levels.
- Depletion of EMI1 partially reverses inhibition of APC/C substrate degradation by E7.

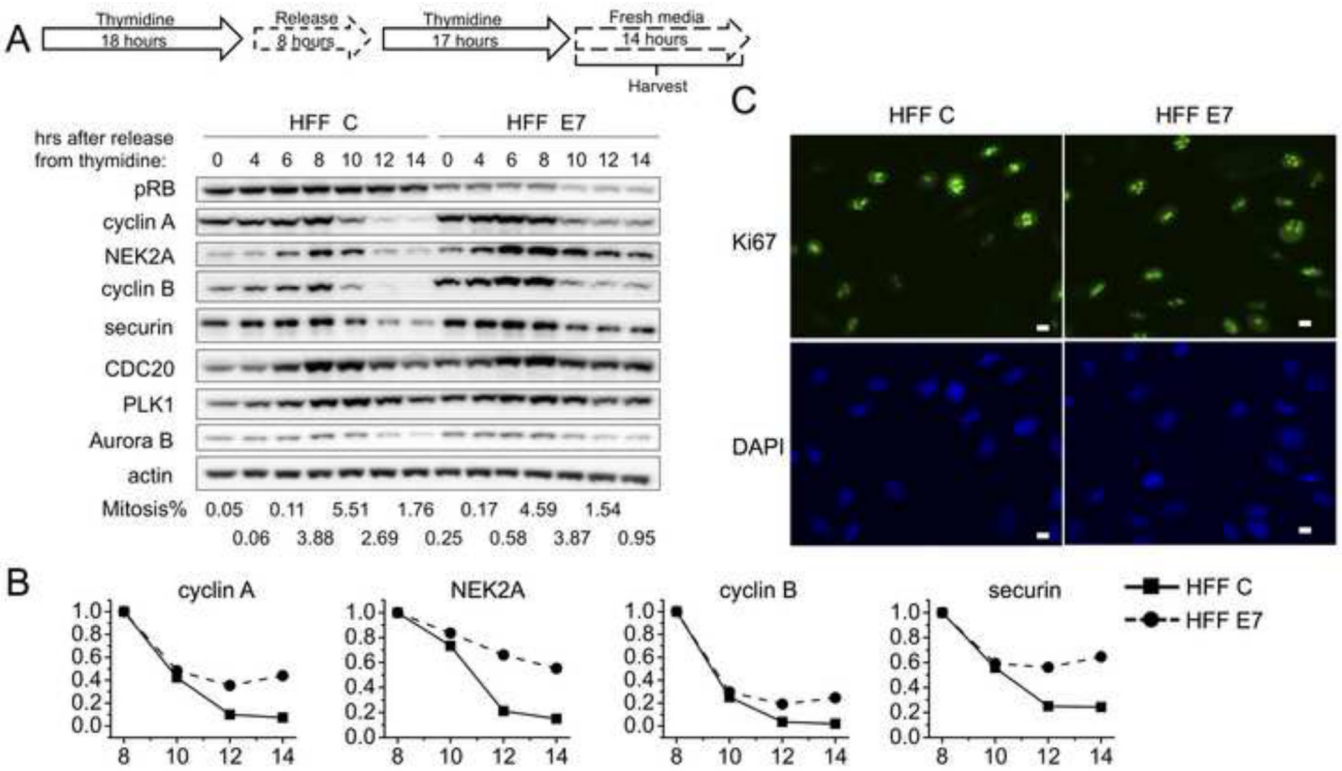

Figure 1. HPV16 E7 expression interferes with the downregulation of a range of APC/C substrates during mitosis in primary human foreskin fibroblasts (HFFs)

(A) HFFs with stable expression of empty vector (HFF C) or HPV16 E7 (HFF E7) were synchronized with a double thymidine block and then released into fresh medium. Protein extracts were prepared at the indicated time points after release from the second thymidine block and steady state levels of pRB, cyclin A, NEK2A, cyclin B, securin, CDC20, PLK1, Aurora B and actin were assessed by Western blotting. The results of a representative experiment are shown. Similar results were obtained in 3 independent experiments. Mitotic indices as determined by FACS analyses with a parallel set of samples stained with MPM-2 and propidium iodide, are presented below the blots. (B) Quantifications of band intensities of cyclin A, NEK2A, cyclin B and securin normalized to actin for the experiment shown in panel A are plotted. Protein levels in HFF C and HFF E7 populations at the 8 hour time points were each set to 1 even though they were not identical in the two cell populations. (C) Representative immunofluorescence analyses of Ki67 in HFF C and HFF E7. Scale bars represent 10 μm.

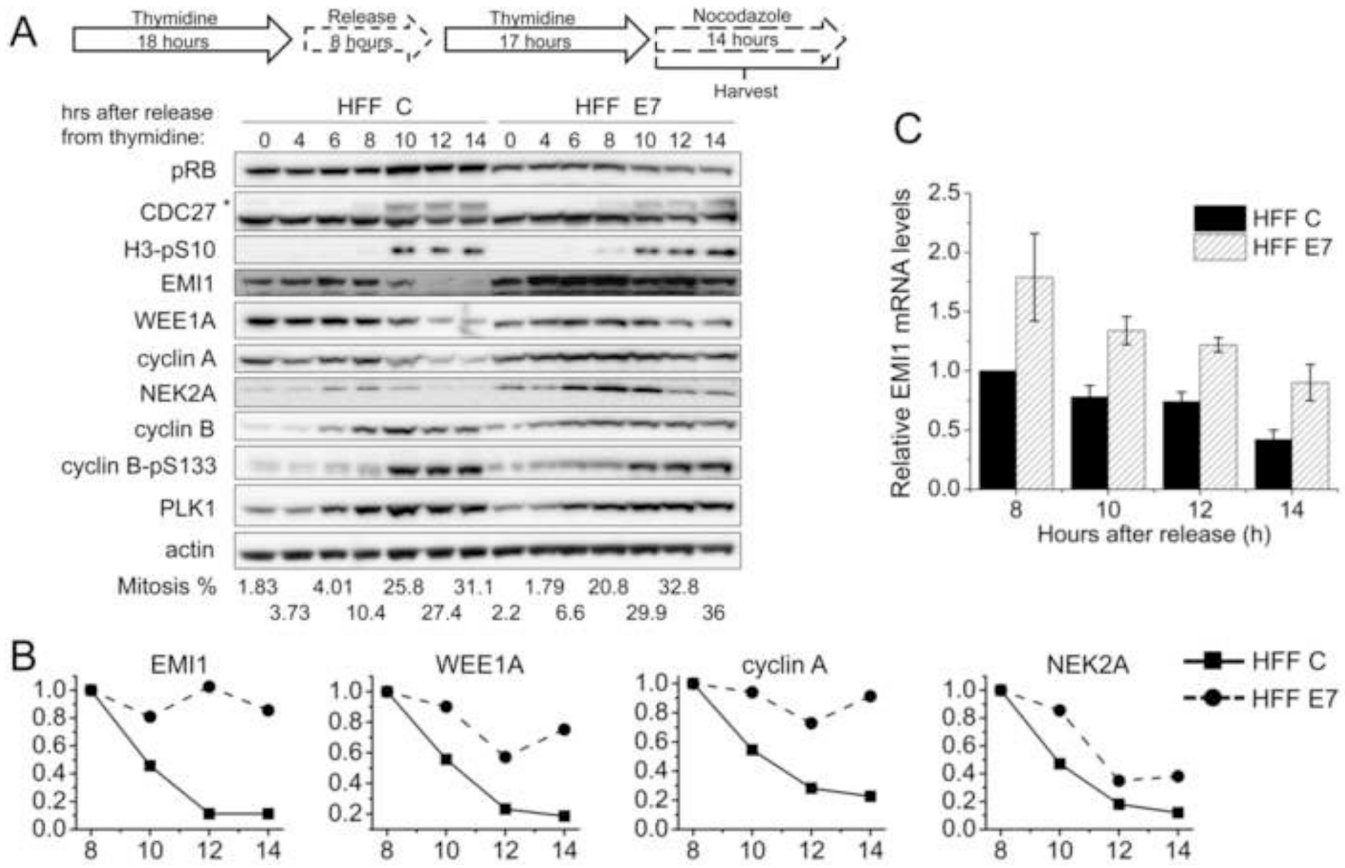

Figure 2. Mitotic EMI1 levels remain high in HPV16 E7-expressing primary human fibroblasts

(A) HFF C and HFF E7 were synchronized with a double thymidine block and then released into 100 ng/ml nocodazole to trap cells in mitosis. Protein extracts were prepared at the indicated time points after release from the second thymidine block into nocodazole. Western blot analyses of pRB, CDC27, histone H3 phosphorylated at serine 10 (H3-pS10), EMI1, WEE1A, cyclin A, NEK2A, cyclin B, cyclin B phosphorylated at serine 133 (cyclin B-pS133), PLK1 and actin are shown. The asterisk in the CDC27 panel indicates slower migrating, phosphorylated form of CDC27. The results of a representative experiment are shown. Similar results were obtained in 5 experiments. Mitotic indices, as determined by FACS analyses with a parallel set of samples stained with MPM-2 and propidium iodide, are presented below the blots. (B) Quantifications of band intensities of EMI1, WEE1A, cyclin A and NEK2A normalized to actin for the experiment presented in panel A are plotted. Protein levels in HFF C and HFF E7 populations at the 8 hour time points were each set to 1 even though they were not identical in the two cell populations. (C) qRT-PCR analyses of EMI1 mRNA expression in HFF C and HFF E7 that were harvested at 8, 10, 12, 14 hours after release from a double thymidine block into nocodazole. The bar graph shows averages and standard deviations from three independent experiments.

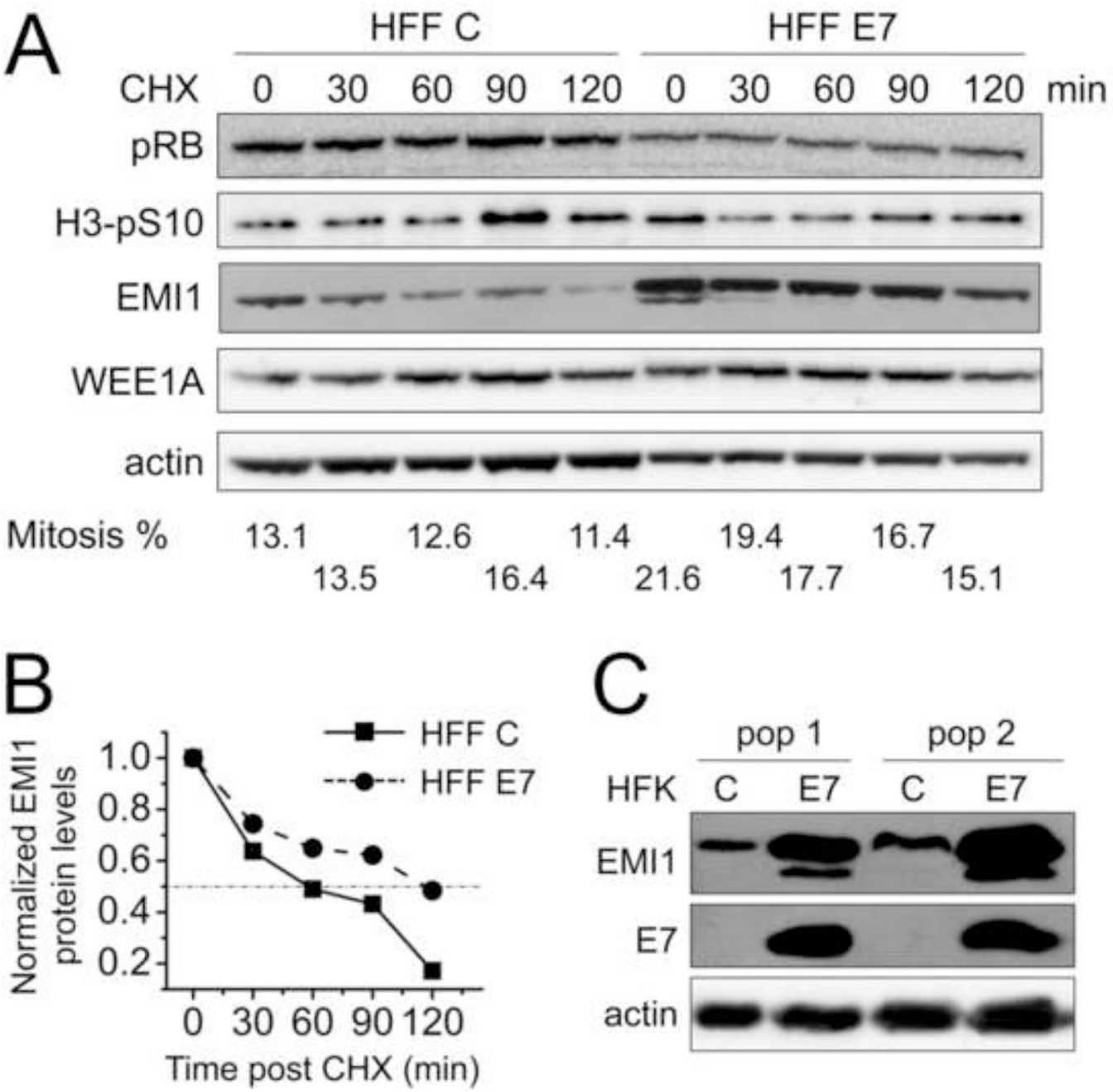

Figure 3. Mitotic EMI1 half-life is increased in HPV16 E7-expressing primary human fibroblasts

(A) HFF C and HFF E7 were arrested in mitosis with 100 ng/ml nocodazole for 18 hours and 25 μg/ml cycloheximide was added to the medium to stop protein translation. Protein extracts were prepared at the indicated time points and steady state levels of EMI1 and WEE1A were determined by Western blotting. The levels of pRB, H3-pS10 and actin are also shown. Twice the amount lysate was analyzed for HFF C so as to render the initial EMI1 levels more comparable to those detected in HFF E7. The results of a representative experiment are shown. Similar results were obtained in two additional independent experiments. Mitotic indices, as determined by FACS analyses with a parallel set of samples stained with MPM-2 and propidium iodide, are presented below the blots. (B)

Quantifications of EMI1 levels normalized to actin for the experiment presented in panel A are plotted. Protein levels in HFF C and HFF E7 populations at the 0 minute time points were each set to 1 even though they were not identical in the two cell populations. (C) Steady state levels of EMI1 as well as E7 and actin were determined by Western blotting in two independently derived human foreskin keratinocyte (HFK) populations with stable expression of HPV16 E7 (E7) or infected with control vector (C).

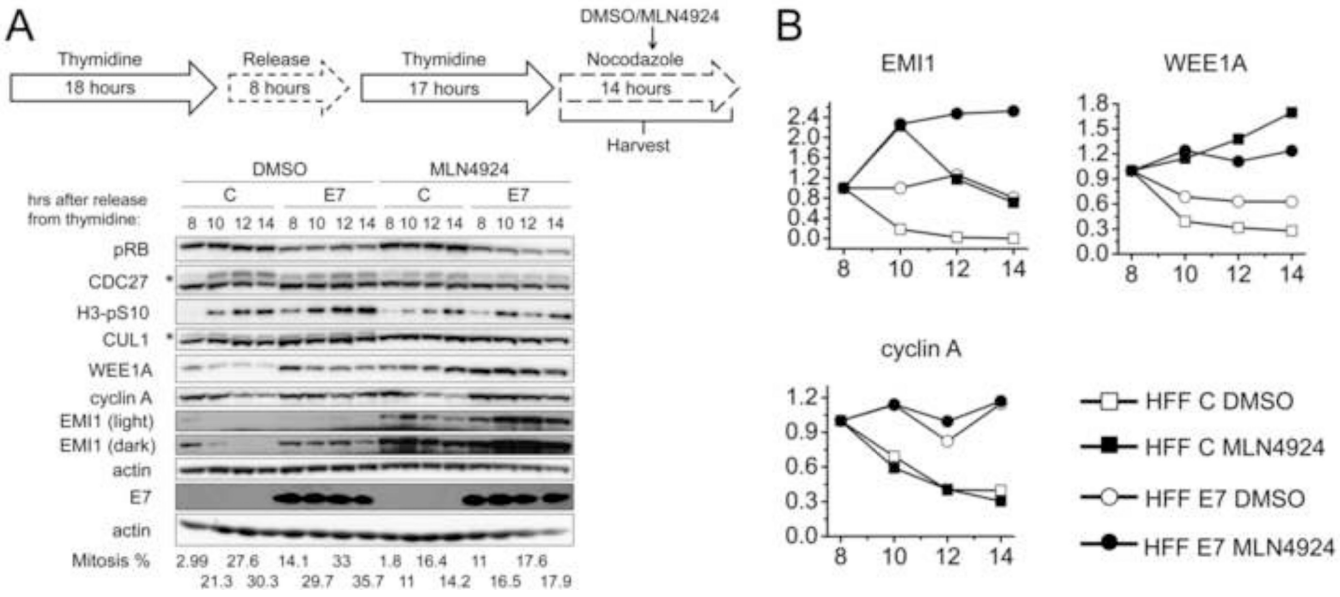

Figure 4. MLN4924 less efficiently stabilizes EMI1 in HPV16 E7-expressing primary human fibroblasts as compared to control cells

(A) HFF C (C) and HFF E7 (E7) were synchronized with a double thymidine block and then released into 100 ng/ml nocodazole to trap cells in mitosis. 1 μM MLN4924 or DMSO was added to the medium at 7.5 hours after release into nocodazole. Protein extracts were prepared at 0.5, 2.5, 4.5, 6.5 hours after MLN4924/DMSO treatment, corresponding to 8, 10, 12, 14 hours after release into nocodazole. Western blot analyses of pRB, CDC27, H3-pS10, CUL1, EMI1, WEE1A, cyclin A and actin are shown. The asterisk in the CDC27 panel indicates slower migrating, phosphorylated form of CDC27 and the asterisk in the CUL1 panel indicates slower migrating, presumably the NEDD8-conjugated form of CUL1. Steady state levels of E7 were determined by Western blotting on a separate gel where 5 times more of the same lysate was analyzed. The results of a representative experiment are shown. Similar results were obtained in two additional independent experiments. Mitotic indices, as determined by FACS analyses with a parallel set of samples stained with MPM-2 and propidium iodide, are presented below the blots. (B) Quantifications of band intensities of EMI1, WEE1A and cyclin A normalized to actin for the experiment shown in panel A are plotted. For each cell population and treatment group protein levels at the 8 hour time points were each set to 1 even though they were identical in the different populations.

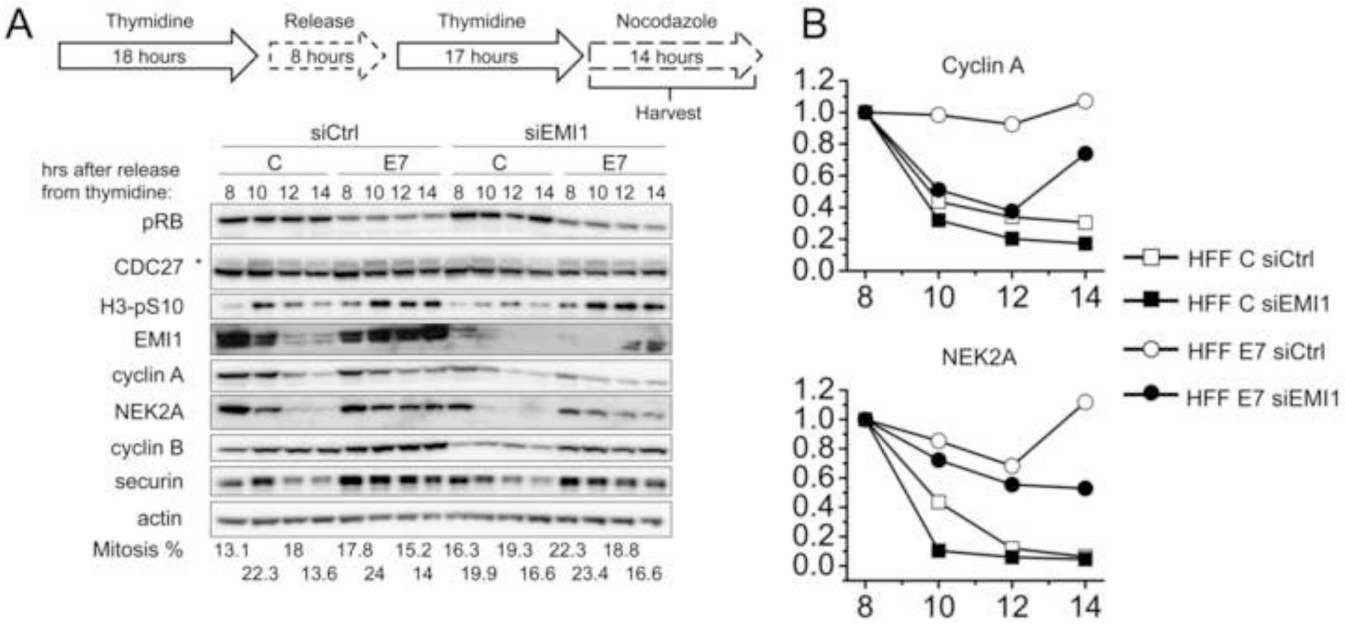

Figure 5. Depletion of EMI1 partially restores degradation kinetics of cyclin A and NEK2A in HPV16 E7-expressing primary human fibroblasts

(A) HFF C (C) and HFF E7 (E7) were transfected with a pool of EMI1 specific siRNAs (siEMI1) or non-targeting control si RNA (siCtrl) before being subjected to a double thymidine block. Cells were then released into nocodazole and protein extracts were prepared at the time points indicated. Western blot analyses of pRB, CDC27, H3-pS10, EMI1, cyclin A, NEK2A, cyclin B, securin and actin are shown. The asterisk in the CDC27 panel indicates slower migrating, phosphorylated form of CDC27. Similar results were obtained in two additional independent experiments. Mitotic indices, as determined by FACS analyses with a parallel set of samples stained with MPM-2 and propidium iodide, are presented below the blots. (B) Quantifications of band intensities of cyclin A and NEK2A normalized to actin for the experiments shown in panel A are plotted. For each cell population and transfection group protein levels at the 8 hour time points were each set to 1 even though they were not identical in the different populations.